CDF note 10120

Measurement of the Polarization Amplitudes of the $B_s^0 \to \phi\phi$ Decay

The CDF Collaboration
URL http://www-cdf.fnal.gov

(Dated: March 31, 2010)

We present the first measurement of the polarization amplitudes for the $B_s^0 \to \phi\phi$ decay. The result is achieved performing an unbinned Maximum Likelihood fit to the Tevatron data collected by the upgraded Collider Detector at Fermilab (CDF II) in the period starting from March 2001 till April 2008, which corresponds to an integrated luminosity of 2.9 fb^{-1}. The yield consists of approximately 300 signal events.

The three estimated polarization amplitudes and the cosine of the strong parallel phase are:

$$|A_0|^2 = 0.348 \pm 0.041(\text{stat}) \pm 0.021(\text{syst})$$
$$|A_\parallel|^2 = 0.287 \pm 0.043(\text{stat}) \pm 0.011(\text{syst})$$
$$|A_\perp|^2 = 0.365 \pm 0.044(\text{stat}) \pm 0.027(\text{syst})$$
$$\cos\delta_\parallel = -0.91^{+0.15}_{-0.13}(\text{stat}) \pm 0.09(\text{syst})$$

and the resulting polarization fractions are:

$$f_{\text{L}} = 0.348 \pm 0.041(\text{stat}) \pm 0.021(\text{syst})$$
$$f_{\text{T}} = 0.652 \pm 0.041(\text{stat}) \pm 0.021(\text{syst})$$

We perform the same analysis for the $B_s^0 \to J\psi\phi$ decay as well, used as control sample. The polarizations amplitudes we find are consistent with the published ones [1].

I. INTRODUCTION

The $B_s^0 \to \phi\phi$ decay proceeds through a $b \to s\bar{s}s$ quark level process, and, in the Standard Model (SM), the dominant diagram is the $b \to s$ penguin (see FIG. 1). The same penguin amplitude is also relevant for several observables which have shown interesting deviation from the SM predictions like the difference in partial rate CP asymmetries in $B_d \to K^+\pi^-$ and $B^+ \to K^+\pi^0$ or the possible, albeit presently not significant, difference in the measurement of $sin(2\beta)$ in $b \to s\bar{q}q$ and in $b \to c\bar{c}s$ B^0 decays. Similar comparison between $sin(2\beta_s)$ measurements in $B_s^0 \to \phi\phi$ and $B_s^0 \to J/\psi\phi$ modes will be possible in the future. The first step in this direction is the measurement of the polarization in the $B_s^0 \to \phi\phi$ decay described here.

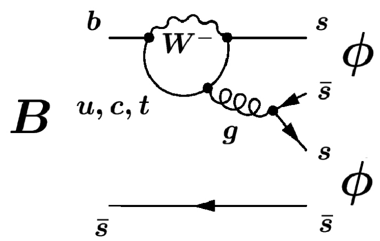

FIG. 1: $B_s^0 \to \phi\phi$ Feynman graph

The decay amplitude for this decay, involving two vector meson in the final state, can be expressed in terms of three independent decay amplitudes, which correspond to the three possible relative angular momenta L between the vector mesons [30]. Different formalisms could be involved in this description; the most suitable one makes use of three *polarization* amplitudes (one longitudinal, $|A_0|^2$, and two transverse, $|A_\parallel|^2$ and $|A_\perp|^2$), which can be measured from an analysis of the emission angles of the final states particles (*i. e.*, the products from the V mesons decays. Since the final-state with a definite angular momentum is a CP-eigenstate, this decomposition allows one to investigate the B_s^0 system CP-properties in the interference between decay and mixing and to measure the B_s^0 decay width difference ($\Delta\Gamma_s$).

Taking in to account the V-A nature of weak interaction and the helicity conservation in QCD, the expectation is that the three amplitudes result in a dominant longitudinal polarization with the transversely-polarized amplitudes suppressed by a factor m_V/m_B [2]. While this is experimentally confirmed in the tree-level dominated $b \to u$ transition (such as $B^0 \to \rho^+\rho^-$ [3, 4], $B^+ \to \rho^0\rho^+$ [5], and $B^+ \to \omega\rho^+$ [6]) and there is evidence in $b \to d$ penguin transition ($B^0 \to \rho^0\rho^0$ [7]), in $B \to \phi K^\star$, a $\bar{b} \to \bar{s}$ penguin decay, it has been measured that the transverse polarization is about equal to the longitudinal one [8–10]. This surprising result is known as "Polarization Puzzle". It is then important to experimentally check what happen in other $\bar{b} \to \bar{s}$ penguin dominated decays like $B_s^0 \to \phi\phi$. Explanation involving either New Physics [11, 12] or corrections to naive expectation within the Standard Model involving either penguin annihilation [2, 13, 14] or final state interactions [15–18], have been proposed. Moreover, within the penguin annihilation hypothesis it is possible to derive predictions for the $B_s^0 \to \phi\phi$ mode based on experimental information in SU(3) related B^0 modes and an estimate of SU(3) breaking[19].

In this report we present the first measurement of $B_s^0 \to \phi\phi$ polarization amplitudes using 2.9 fb^{-1}of CDF II data, corresponding to a signal yield of about 300 events. In the same sample we have measured the branching ratio of the $B_s^0 \to \phi\phi$ decay [21], which is in agreement with the published measurement from CDF based on only 180 pb^{-1}[20].

We also present the polarization amplitudes measurement of the $B_s^0 \to J/\psi\phi$ decays as well, in a data sample selected with the same trigger selections of the $B_s^0 \to \phi\phi$ decay. Since the $B_s^0 \to J\psi\phi$ decay properties are well known, this decay constitutes a powerful control sample.

Note that charge conjugate decay modes are implied throughout the rest of this document unless otherwise stated.

II. $P \to VV$ DECAY RATE

In this section we report the description of the differential decay rate as function of the angles and time. The two complete decay chains considered are $B_s^0 \to \phi\phi \to [K^+K^-][K^+K^-]$ and $B_s^0 \to J/\psi\phi \to [\mu^+\mu^-][K^+K^-]$. We refer to the B_s^0 meson as the parent (or as the initial state) and to the two vector mesons as daughter particles (V_1 and V_2), and to their decay products as final state particles (P_1, P_2 from V_1, and P_3, P_4 from V_2) [31].

A. $B_s^0 \to \phi\phi$

In the $B_s^0 \to \phi\phi$ decay the daughters state are identical bosons; the natural angular basis satisfying Bose statistics comes from the helicity formalism: the x' (x'') axis is defined as the direction of the V_1 (V_2) momentum in the rest frame of the B_s^0; we define ϑ_1 (ϑ_2) as the angle between the x' (x'') axis and the P_1 (P_3) three-momentum vector, defined in the rest frame of their mother V_1 (V_2); the Φ angle is the angle between the decay planes of the two daughter particles. These angles, which form the vector $\vec{\omega} = (\cos\vartheta_1, \cos\vartheta_2, \Phi)$, are shown in FIG. 2.

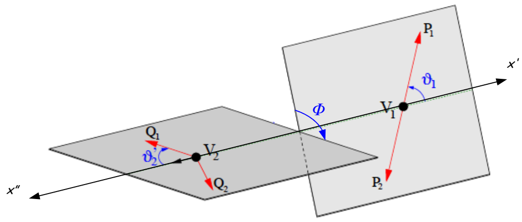

FIG. 2: Definitions of the helicity angles $\vec{\omega} = (\vartheta_1, \vartheta_2, \Phi)$ for a general $P \to V_1V_2$ decay. We identify $B_s \to \phi\phi \to [K^+K^-][K^+K^-]$ with $P \to V_1V_2 \to [P_1P_2][Q_1Q_2]$.

The differential decay rate in terms of the helicity angles can be written as

$$\frac{d^4\Lambda(\vec{\omega}, t)}{dt d\vec{\omega}} = \frac{9}{32\pi}\sum_{i=1}^{6} K_i(t) f_i(\vec{\omega}) \tag{1}$$

where the angular functions $f_i(\vec{\omega})$ are given by

$$\begin{aligned} f_1(\vec{\omega}) &= 4\cos^2\vartheta_1\cos^2\vartheta_2 \\ f_2(\vec{\omega}) &= \sin^2\vartheta_1\sin^2\vartheta_2(1+\cos 2\Phi) \\ f_3(\vec{\omega}) &= \sin^2\vartheta_1\sin^2\vartheta_2(1-\cos 2\Phi) \\ f_4(\vec{\omega}) &= -2\sin^2\vartheta_1\sin^2\vartheta_2\sin 2\Phi \\ f_5(\vec{\omega}) &= \sqrt{2}\sin 2\vartheta_1\sin 2\vartheta_2\cos\Phi \\ f_6(\vec{\omega}) &= -\sqrt{2}\sin 2\vartheta_1\sin 2\vartheta_2\sin\Phi \end{aligned} \tag{2}$$

while the time-dependent functions $K_i(t)$ are defined as

$$
\begin{aligned}
K_1(t) =& \frac{1}{2}|A_0|^2 \Bigg[(1+\cos\phi_\mathrm{s})e^{-\Gamma_\mathrm{L}t} + (1-\cos\phi_\mathrm{s})e^{-\Gamma_\mathrm{H}t} + 2e^{-\Gamma t}\sin(\Delta m t)\sin\phi_\mathrm{s}\Bigg] \\
K_2(t) =& \frac{1}{2}|A_\parallel|^2 \Bigg[(1+\cos\phi_\mathrm{s})e^{-\Gamma_\mathrm{L}t} + (1-\cos\phi_\mathrm{s})e^{-\Gamma_\mathrm{H}t} + 2e^{-\Gamma t}\sin(\Delta m t)\sin\phi_\mathrm{s}\Bigg] \\
K_3(t) =& \frac{1}{2}|A_\perp|^2 \Bigg[(1-\cos\phi_\mathrm{s})e^{-\Gamma_\mathrm{L}t} + (1+\cos\phi_\mathrm{s})e^{-\Gamma_\mathrm{H}t} - 2e^{-\Gamma t}\sin(\Delta m t)\sin\phi_\mathrm{s}\Bigg] \\
K_4(t) =& |A_\parallel||A_\perp| \Bigg[e^{-\Gamma t}\Bigg(\sin(\delta_\perp-\delta_\parallel)\cos(\Delta m t) - \cos(\delta_\perp-\delta_\parallel)\sin(\Delta m t)\cos\phi_\mathrm{s}\Bigg) - \\
& - \frac{1}{2}\Bigg(e^{-\Gamma_\mathrm{H}t} - e^{-\Gamma_\mathrm{L}t}\Bigg)\cos(\delta_\perp-\delta_\parallel)\sin\phi_\mathrm{s}\Bigg] \\
K_5(t) =& \frac{1}{2}|A_0||A_\parallel|\cos(\delta_\parallel) \\
& \Bigg[(1+\cos\phi_\mathrm{s})e^{-\Gamma_\mathrm{L}t} + (1-\cos\phi_\mathrm{s})e^{-\Gamma_\mathrm{H}t} + 2e^{-\Gamma t}\sin(\Delta m t)\sin\phi_\mathrm{s}\Bigg] \\
K_6(t) =& |A_0||A_\perp| \Bigg[e^{-\Gamma t}\Bigg(\sin\delta_\perp\cos(\Delta m t) - \cos\delta_\perp\sin(\Delta m t)\cos\phi_\mathrm{s}\Bigg) - \\
& - \frac{1}{2}\Bigg(e^{-\Gamma_\mathrm{H}t} - e^{-\Gamma_\mathrm{L}t}\Bigg)\cos\delta_\perp\sin\phi_\mathrm{s}\Bigg]
\end{aligned} \tag{3}
$$

The time-dependent angular distribution for a $\bar{B}_s^0$ meson can be obtained by reversing the sign of the terms proportional to $\sin(\Delta m t)$ or $\cos(\Delta m t)$ in the $K_i(t)$ functions. The symbols are defined in the following:

- the three *polarization amplitudes* are $|A_0|^2$, $|A_\parallel|^2$ and $|A_\perp|^2$;
- we denote the masses and widths of the two mass eigenstates with $M_\mathrm{H,L}$ and $\Gamma_\mathrm{H,L}$ and define $\Delta m = M_\mathrm{H} - M_\mathrm{L}$, $\Gamma = 1/\tau_B = (\Gamma_\mathrm{L} + \Gamma_\mathrm{H})/2$ and $\Delta\Gamma = \Gamma_\mathrm{L} - \Gamma_\mathrm{H}$; the last update results [22] for B_s meson are: $\tau_\mathrm{L} = 1/\Gamma_\mathrm{L} = 1.408^{+0.033}_{-0.030}$ ps, $\tau_\mathrm{H} = 1/\Gamma_\mathrm{H} = 1.543^{+0.058}_{-0.060}$ ps and $\Delta\Gamma_s = 0.062^{+0.034}_{-0.037}\,\mathrm{ps}^{-1}$.
- The phase ϕ_s is the physical phase related to the CP violation; in the SM, it is predicted to be very small [23], $\phi_\mathrm{s}^\mathrm{SM} = 0.0041 \pm 0.0008$.
- We define the two strong phases: $\delta_\parallel = \arg(A_0^\star A_\parallel)$ and $\delta_\perp = \arg(A_0^\star A_\perp)$.

Assuming that:

1. we are not able to distinguish a B_s^0 meson from a $\bar{B}_s^0$ meson and thus we have to sum over the B_s^0 and $\bar{B}_s^0$ terms of distribution [32];
2. we are not sensitive in measuring ϕ_s and we assume its value in the SM [33], thus we fix $\phi_\mathrm{s} = 0$ in the $K_i(t)$ functions;

then the differential angular decay rate of eq. 1 becomes

$$\frac{d^4\Lambda(\vec{\omega},t)}{dt d\vec{\omega}} = \frac{9}{32\pi}\Bigg[\mathcal{F}_\mathrm{e}(\vec{\omega})\mathcal{K}_\mathrm{L}(t) + \mathcal{F}_\mathrm{o}(\vec{\omega})\mathcal{K}_\mathrm{H}(t)\Bigg] \tag{4}$$

where we distinct two time-dependent and two angular-dependent terms:

$$\mathcal{F}_\mathrm{e}(\vec{\omega}) = |A_0|^2 f_1(\vec{\omega}) + |A_\parallel|^2 f_2(\vec{\omega}) + |A_0||A_\parallel|\cos\delta_\parallel f_5(\vec{\omega}) \tag{5a}$$
$$\mathcal{F}_\mathrm{o}(\vec{\omega}) = |A_\perp|^2 f_3(\vec{\omega}) \tag{5b}$$
$$\mathcal{K}_\mathrm{L}(t) = 2e^{-\Gamma_\mathrm{L}t} \tag{5c}$$
$$\mathcal{K}_\mathrm{H}(t) = 2e^{-\Gamma_\mathrm{H}t} \tag{5d}$$

A comment on eq. 4:

- $\mathcal{F}_{\rm e}(\vec{\omega}) \sim |\langle {\rm f}|B_{\rm L}\rangle|^2$ represents the probability to find the $|\phi\phi\rangle$ state with $L = 0$ or $L = 2$ (S- or D-wave): $\mathsf{CP}\,|\phi\phi\rangle = (-1)^L\,|\phi\phi\rangle = |\phi\phi\rangle$, then $\mathsf{CP}\,|B_{\rm L}\rangle = |B_{\rm L}\rangle$; the light mass (short-lived) eigenstate is also a CP-even eigenstate.
- $\mathcal{F}_{\rm o}(\vec{\omega}) \sim |\langle {\rm f}|B_{\rm H}\rangle|^2$ represents the probability to find the $|\phi\phi\rangle$ state with $L = 1$: $\mathsf{CP}\,|\phi\phi\rangle = (-1)^L\,|\phi\phi\rangle = -\,|\phi\phi\rangle$, then $\mathsf{CP}\,|B_{\rm H}\rangle = -\,|B_{\rm H}\rangle$; the heavy mass (long-lived) eigenstate is also a CP-odd eigenstate.

B. $B_s^0 \to J/\psi\phi$

The customary choice for the $B_s^0 \to J/\psi\phi$ angular analysis is the transversity basis. The three transversity angles form the angles vector $\vec{\Omega} = (\Theta, \Psi, \Phi)$, and they are defined as follow. In the rest frame of V_1, V_2 moves in the x direction, and the z axis is perpendicular to the decay plane of $V_2 \to P_3P_4$ and we assume that the y-component of the P_3 three-momentum is non-negative. (Θ, Φ) are the angular coordinates of P_1 and Ψ is that of P_2, both in the rest frame of V_1 (see FIG. 3).

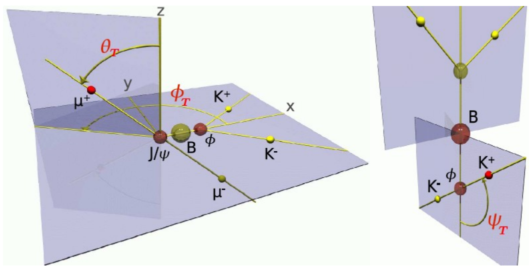

FIG. 3: Definitions of the transversity angles.

The differential angular decay rate has the same form of eq. 1, with the $f_i(\vec{\Omega})$ functions defined by:

$$
\begin{aligned}
f_1(\vec{\Omega}) &= 4\cos^2\Psi(1 - \sin^2\Theta\cos^2\Phi)\\
f_2(\vec{\Omega}) &= \sin^2\Psi(1 - \sin^2\Theta\sin^2\Phi)\\
f_3(\vec{\Omega}) &= \sin^2\Psi\sin^2\Theta\\
f_4(\vec{\Omega}) &= -\sin^2\Psi\sin 2\Theta\sin\Phi\\
f_5(\vec{\Omega}) &= \frac{1}{\sqrt{2}}\sin 2\Psi\sin^2\Theta\sin 2\Phi\\
f_6(\vec{\Omega}) &= \frac{1}{\sqrt{2}}\sin 2\Psi\sin 2\Theta\cos\Phi
\end{aligned}
\tag{6}
$$

and replacing $\phi_{\rm s}$ with $2\beta_s$ in the $K_i(t)$ terms. As for $B_s^0 \to \phi\phi$, if we sum over B_s^0 and $\bar{B}_s^0$ terms and assume for β_s the SM value ($\beta_s \simeq 0$), we get the analogous distribution for $B_s^0 \to J/\psi\phi$ as the one described by eq. 4.

III. DETECTOR TRIGGER AND DATA SAMPLE

The CDF II detector is described in detail elsewhere [?]. Most relevant to this analysis are the tracking and trigger systems. Hadronic B decays are collected via a dedicated track trigger capable of identifying tracks displaced from the primary vertex due to the long lifetime of b-hadrons. The online track reconstruction is performed first in the central drift chamber (COT) by the XFT track processor [24] and by the Silicon Vertex Tracker [?] at the second level trigger. The latter combines the drift chamber and silicon vertex informations achieving impact parameter resolution similar to offline.

The analysis described here uses a data sample selected requiring two charged tracks with transverse momenta $p_T \geq 2$ GeV/c and with impact parameter 120 μm $\leq d_0 \leq$ 1000 μm. Furthermore the two trigger tracks must have an opening angle in the transverse plane satisfying $2^\circ \leq |\Delta\phi| \leq 90^\circ$ and must satisfy the requirement $L_{xy} \geq 200$ μm, where the two dimensional decay length, L_{xy}, is calculated as the transverse distance from the beam line to the two track vertex projected along the total transverse momentum of the track pair. FIG. 4 shows a sketch of the relevant kinematic variables used.

Three slightly different requirements on the scalar sum of track transverse momenta, $p_{T1} + p_{T2}$, define the three subsamples used for this measurement. That is `B_CHARM_LOWPT` requires $p_{T1} + p_{T2} > 4$ GeV/c, `B_CHARM_L1` ask for opposite charge tracks and $p_{T1} + p_{T2} > 5.5$ GeV/c while `B_CHARM_HIGHPT` ask for opposite charge tracks with $p_{T1} + p_{T2} > 6.5$ GeV/c. The three different subsample are combined together after taking in to account the different effective luminosity integrated by each of them due to varying trigger prescale factor applied online in order to keep the total trigger rate manageable.

In the following we will refer to *exclusive* trigger configurations. These are defined as follow:

- `HIGHPT`: only `B_CHARM_HIGHPT`;
- `ScA` (Scenario A) : events selected by `B_CHARM_L1` and not by `B_CHARM_HIGHPT`
- `LOWPT`: events selected by `B_CHARM_LOWPT` but not by both `B_CHARM_L1` and `B_CHARM_HIGHPT`.

Their percentages on the total sample are listed in TAB. I for both decays. We request the matching between at least two reconstructed tracks and the SVT tracks. The confirmation of the `B_CHARM_LOWPT` trigger selections is imposed.

Trigger Paths	Fractions	
	$B_s^0 \to \phi\phi$	$B_s^0 \to J/\psi\phi$
`HIGHPT`	0.39 ± 0.05	0.42 ± 0.02
`ScA`	0.38 ± 0.05	0.33 ± 0.02
`LOWPT`	0.22 ± 0.04	0.26 ± 0.02

TABLE I: Trigger paths fractions (exclusive selection).

Planar drift chambers [?] are used to identify muons with different transverse momentum thresholds due to geometry and material in front of them. For pseudo-rapidity $\eta \lesssim 0.6$ the CMU and CMP chambers [? ?] can identify muons with $p_T > 1.5$ GeV/c, while for pseudo-rapidity $0.6 \lesssim \eta \lesssim 1.0$ CMX chambers [?] have a threshold of approximately 2 GeV/c.

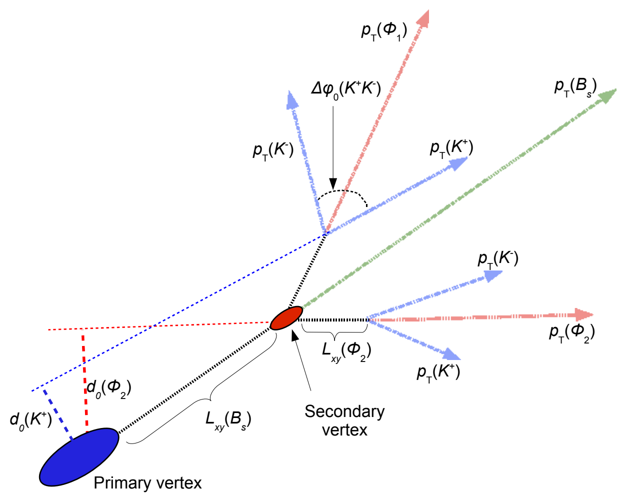

FIG. 4: Sketch of the$B_s^0 \to \phi\phi \to [K^+K^-][K^+K^-]$ decay projected into the transverse plane. Ellipses indicate vertexes, arrows indicate the transverse momenta (*i. e.*, the direction) of charged particles. Nothing is to scale.

The sample has been collected in the data taking period from beginning of Run II till April 2008, and the integrated luminosity (without accounting for prescale factors) is 2.9 ± 0.2 fb^{-1}. We reconstruct the two body B_s^0 decay to two $\phi(1020)$ vector mesons with $\phi(1020) \rightarrow K^+K^-$ (BR=$49.2 \pm 0.6\%$ [22]), the final states thus consists of 4 charged kaons emerging from a single displaced vertex. We reconstruct the $B_s^0 \rightarrow J/\psi\phi$ decay using $J/\psi \rightarrow \mu^+\mu^-$ and $\phi(1020) \rightarrow K^+K^-$ decays leading in a $\mu^+\mu^-K^+K^-$ combination again from a single displaced vertex. To reconstruct B_s^0candidate all four-track combinations that satisfy trigger criteria are fit to a common vertex. All the tracks that are used in the vertex fit are required to have both drift chamber and silicon vertex hits and a minimum transverse momentum of 400 MeV/c.

Opposite charge track pairs with invariant mass within 15 MeV/c^2 from the PDG [22] $\phi(1020)$ mass are considered $\phi(1020)$ candidates. In the case of $B_s^0 \rightarrow J/\psi\phi$ vertex fit a mass constraint is also employed, imposing for the two muon candidates from J/ψ decay that their invariant mass is equal to the J/ψ world average mass. This mass constraint significantly improves the invariant mass resolution of the measured $\mu^+\mu^-K^+K^-$ mass. At least one of the two muons from the J/ψ decay is required to have a confirmation in the muon detectors located outside of the calorimeters which can detect muons with momentum above 1.5 GeV/c. With this requirements an abundant and clean sample of $B_s^0 \rightarrow J/\psi\phi$ events is collected, keeping to a negligible level the contamination from $J/\psi \rightarrow e^+e^-$ decays. The selected $B_s^0 \rightarrow J/\psi\phi$ sample with just one muon leg identified is an interesting sample per se since it identify a largely independent sample with respect to the one collected with the dedicated J/ψ triggers and used for the most precise $\Delta\Gamma_s$ and β_s measurements to date [**?**].

IV. OPTIMIZATION PROCEDURE

Huge backgrounds due to random track combinations and to ϕ production from heavy flavor decays combined with two other random tracks need to be reduced in order to identify the $B_s^0 \rightarrow \phi\phi$ and the $B_s^0 \rightarrow J/\psi\phi$ signals. We inherit the set of cuts on discriminating variables form the BR analysis [21], since we see that having the same signal selection for both the BR and the polarization measurements is acceptable and it is foreseeable that no big improvement should come from a more specific selection optimization. Thus, we point to [21] for details on the optimization procedure and we report here only the resulting selection with the discriminating variables. The latter are only kinematic variables:

- for the $B_s^0 \rightarrow \phi\phi$ decay:
  - L_{xy}^B: transverse decay length of the reconstructed B;
  - d_0^B: impact parameter of the reconstructed B;
  - $d_0^{\phi_{\max}}$: impact parameter of the ϕ with higher momentum;
  - $p_{\mathrm{T}\,\min}^K$: transverse momentum of the softer kaon;
  - χ^2_{xy}: χ^2 of the fit used in the reconstruction of the secondary vertex;
- for the $B_s^0 \rightarrow J/\psi\phi$ decay:
  - L_{xy}^B: transverse decay length of the reconstructed B;
  - d_0^B: impact parameter of the reconstructed B;
  - p_T^ϕ: transverse momentum of the ϕ;
  - $p_\mathrm{T}^{J/\psi}$: transverse momentum of the J/ψ;
  - χ^2_{xy}: χ^2 of the fit used in the reconstruction of the secondary vertex;

The optimized cuts for the two signals selections are summarized in TAB. II.

V. THE FINAL DATA SAMPLE

Applying the cuts listed in TAB. II, the invariant mass distributions, $m_{K^+K^-K^+K^-}$ for the $B_s^0 \rightarrow \phi\phi$ and $m_{K^+K^-\mu^+\mu^-}$ for the $B_s^0 \rightarrow J/\psi\phi$, are obtained (FIG. 5). These provides us with a first insight on the background and signal composition. In these distributions at least three components can be identified:

the signal: we have the following number of signal events:

Variables		Requirements	
		$B_s^0 \to \phi\phi$	$B_s^0 \to J/\psi\phi$
L_{xy}^B	[μm]	> 330	> 290
$p_{\mathrm{T}\,\min}^K$	[GeV/c]	> 0.7	
p_{T}^{ϕ}	[GeV/c]		> 1.4
χ_{xy}^2		< 17	< 15
d_0^B	[μm]	< 65	< 80
$d_0^{\phi\max}$	[μm]	> 85	
$p_{\mathrm{T}}^{J/\psi}$	[GeV/c]		> 2.0

TABLE II: Optimized selection cuts.

	$B_s^0 \to \phi\phi$	$B_s^0 \to J/\psi\phi$
Yield	295 ± 20	1766 ± 48

These yields are extracted from the binned fit in [21]: the fit function used is the sum of two gaussians (having the same mean value but different resolutions) and a decreasing exponential.

combinatorial background: these are random combinations of charged tracks accidentally satisfying the selection requirements. They produce a continuous invariant B_s^0 mass distribution and we expect a smooth slowing decreasing distribution in the signal region. It is the more important source of background in this analysis.

physics background: it is due to partially reconstructed heavy flavor decays or to an incorrect mass assignment to the tracks of other B meson decays (they are often referred to as *reflections*). We expect a distribution with a peak under the signal:

- for the $B_s^0 \to \phi\phi$: the decays that could produce reflections in the B_s^0 mass window are: $B_d^0 \to \phi K^\star \to [K^+K^-][K^{+(-)}\pi^{-(+)}]$ and $B_s^0 \to \bar{K}^\star K^\star \to [K^{+(-)}\pi^{-(+)}][K^{+(-)}\pi^{-(+)}]$; these reflections occur when the $K^\star$ is incorrectly reconstructed as a ϕ. The estimated number of reflection events is [21]:

	$B_s^0 \to \bar{K}^\star K^\star$	$B_d^0 \to \phi K^\star$
Events	0	8 ± 3
Fraction respect to signal events [%]	10^{-6}	3 ± 1

Since its tiny percentage respect to the signal events, the $B_d^0 \to \bar{K}^\star K^\star$ reflection is neglected.

- for the $B_s^0 \to J/\psi\phi$: the more frequent background decay is the $B_d^0 \to J/\psi K^\star \to [\mu^+\mu^-][K^{+(-)}\pi^{-(+)}]$ decay; it occurs when in the reconstruction the daughter tracks of the $K^\star$ are assumed to be two kaons and an incorrect invariant mass is computed. The estimated number of reflection events is [21]:

	$B_d^0 \to J/\psi K^\star$
Events	70 ± 20
Fraction respect to signal events [%]	4 ± 1

VI. MEASUREMENT OF THE POLARISATION AMPLITUDES

The aim of the analysis is the estimation of the two polarization amplitudes, $|A_0|^2$ and $|A_\parallel|^2$ and the relative strong phase between them, $\delta_\parallel$, using as probability density function (pdf) the angular decay rate distribution of eq. 4 integrated in time. In eq. 4 we fix Γ_{L} and Γ_{H} to the latest PDG values; moreover, the CP-violation's phase ϕ_{s} is set equal to zero and there is no distinction between B_s^0 and $\bar{B}_s^0$ at the production time (*untagged* analysis).

We perform an unbinned Maximum Likelihood (ML) to the following variables:

- the reconstructed mass m of the B_s^0 candidate;
- the reconstructed angles

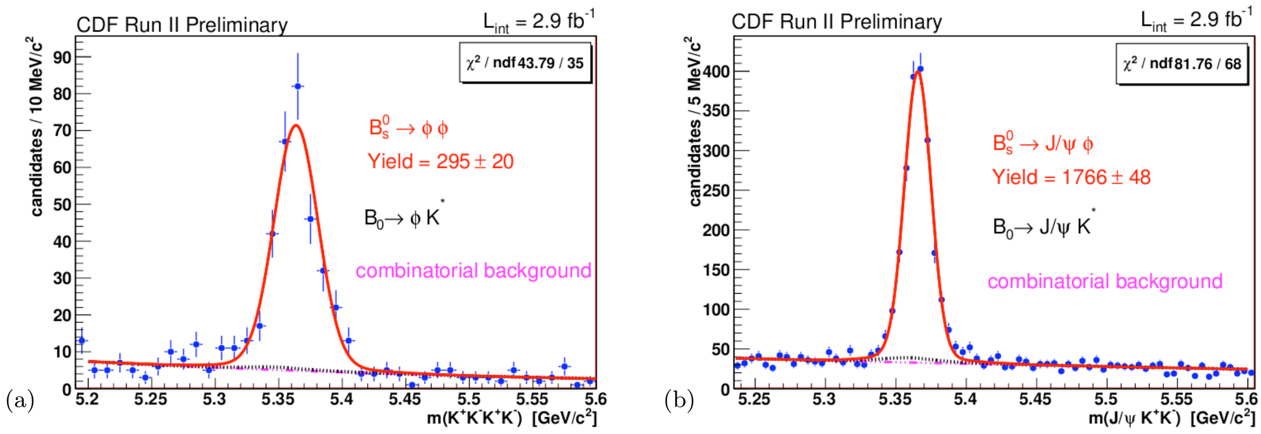

FIG. 5: Signal and background composition in the $B_s^0 \to \phi\phi$ (a) and $B_s^0 \to J/\psi\phi$ (b) decays. The blue points represent data after the optimized selection; the red line is the total fit distribution; in black the reflection component; in purple the combinatorial background.

– in the helicity basis, $\vec{\omega} = (\cos\vartheta_1, \cos\vartheta_2, \varPhi)$, for the $B_s^0 \to \phi\phi$ decay;

– in the transversity basis, $\vec{\Omega} = (\cos\Theta, \cos\Psi, \Phi)$, for the $B_s^0 \to J/\psi\phi$ decay;

The mass distribution is used in the fit to discriminate the signal yield with respect to the background.

In the $B_s^0 \to \phi\phi$ decay, the identification of the two ϕ as ϕ_1 and ϕ_2 (and then of the two angles ϑ_1 and ϑ_2) is randomly implemented in order to carry out the symmetry of the variables under indexes exchange $1 \leftrightarrow 2$. Since the main purpose is the $B_s^0 \to \phi\phi$ angular analysis, in the following all the notations refer to its study, but the same procedure is adopted in the $B_s^0 \to J/\psi\phi$ study with obvious replacements.

The observables m and $\vec{\omega}$ give rise to the event measurements vector $\vec{x}_i = (m_i, \vec{\omega}_i)$, where i spans over the number of events n. The Likelihood function is the product of the pdf g of the parameters vector $\vec{\xi}$ evaluated at each event i,

$$\mathcal{L}(\vec{\xi}) = \prod_{i=1}^{n} g(\vec{x}_i; \vec{\xi}). \tag{7}$$

The pdf is the sum of two components: $g_{\rm s}$, representing the signal set, and $g_{\rm b}$, for the background events, *i. e.*,

$$g(\vec{x}_i, \vec{\xi}) = (1 - f_{\rm b}) g_{\rm s}(\vec{x}_i, \vec{\xi}_{\rm s}) + f_{\rm b} g_{\rm b}(\vec{x}_i, \vec{\xi}_{\rm b}), \tag{8}$$

where $f_{\rm b}$ is the fraction of background events ($0 \leq f_{\rm b} \leq 1$). Since the mass and the angular variables are statistically independent, the pdf can be factorized in two corresponding terms:

$$g_{\rm s}(\vec{x}_i, \vec{\xi}_{\rm s}) = g_{\rm s}^{(m)}(m_i, \vec{\xi}_{\rm s}^{m}) g_{\rm s}^{(\omega)}(\vec{\omega}_i, \vec{\xi}_{\rm s}^{\omega}), \tag{9a}$$

$$g_{\rm b}(\vec{x}_i, \vec{\xi}_{\rm b}) = g_{\rm b}^{(m)}(m_i, \vec{\xi}_{\rm b}^{m}) g_{\rm b}^{(\omega)}(\vec{\omega}_i, \vec{\xi}_{\rm b}^{\omega}) \tag{9b}$$

We evaluate the best parametrization of the pdf components, using also the Monte Carlo (MC) simulation. They are presented in the following sections. This procedure allowed us to fix some parameters in the function parametrization and then to make a global fit with a limited number of free parameters. We don't consider the reflection components in the background parametrization: since they are a tiny percentage of the total data sample, they can be neglected at first order. Thus, if it is not properly pointed out, when we refer to the background, we mean only the dominant combinatorial component.

A. Mass Model

The signal distribution has a width of around 20 MeV/c^2 for the $B_s^0 \to \phi\phi$ and of around 10 MeV/c^2 for the $B_s^0 \to J/\psi\phi$. In both cases, it is parametrized with two gaussian functions having the same mean value M but different resolutions, σ and $k\sigma$. This choice is fairly standard and takes into account the detector effects that cause an additional spread in the tail distributions. The function used to parametrize the distributions is the following:

$$g_{\mathrm{s}}^{(m)} = h\frac{1}{\sqrt{2\pi}\sigma}e^{-\frac{(m-M)^2}{2\sigma^2}} + (1-h)\frac{1}{\sqrt{2\pi}k\sigma}e^{-\frac{(m-M)^2}{2k^2\sigma^2}} \tag{10}$$

where h is the fraction of one gaussian component with respect to the other. In the final fit the multiplicative factor k and the fraction h are fixed from the fit to large MC data sample, while the other parameters are left free.

The mass background follows, with a good approximation, an exponentially decreasing behavior:

$$g_{\mathrm{b}}^{(m)} = \frac{b}{e^{-bm_{\mathrm{min}}} - e^{-bm_{\mathrm{max}}}}e^{-bm} \tag{11}$$

where b is the slope of the exponential function, and m spans the interval $[m_{\mathrm{min}} = 5.2, m_{\mathrm{max}} = 5.6]$ GeV/c^2.

B. Angular Model

The pdf used to describe the helicity angular distribution for the signal is obtained integrating in time the theoretical differential decay rate reported in eq. 4. The resulting signal angular pdf is:

$$g_{\mathrm{s}}^{(\omega)} = \frac{d^3\Lambda(\vec{\omega})}{d\vec{\omega}} = \frac{9}{32\pi}\frac{1}{\tilde{W}}\left[\tilde{\mathcal{F}}_{\mathrm{e}}(\vec{\omega}) + \tilde{\mathcal{F}}_{\mathrm{o}}(\vec{\omega})\right] \tag{12}$$

where

$$\tilde{\mathcal{F}}_{\mathrm{e}} = \frac{2}{\Gamma_{\mathrm{L}}}\left[|A_0|^2 f_1(\vec{\omega}) + |A_\parallel|^2 f_2(\vec{\omega}) + |A_0||A_\parallel|\cos\delta_\parallel f_5(\vec{\omega})\right] \tag{13a}$$

$$\tilde{\mathcal{F}}_{\mathrm{o}} = \frac{2}{\Gamma_{\mathrm{H}}}|A_\perp|^2 f_3(\vec{\omega}) \tag{13b}$$

$$\tilde{W} = \frac{|A_0|^2 + |A_\parallel|^2}{\Gamma_{\mathrm{L}}} + \frac{|A_\perp|^2}{\Gamma_{\mathrm{H}}} \tag{13c}$$

We expect not to have a uniform acceptance in the helicity (transversity) angles. So it is crucial for the analysis to be able to deal with this effect, we refer to as "angular acceptance". The detector acceptance in the angular variables is determined with MC simulation and it is assumed unrelated to the B_s^0 meson proper decay time. The simulated events are passed through the full-fledged detector simulation. Then, they are selected with the same on-line and off-line requirements of the real data. In practice, we construct the three-dimensional acceptance as a three-dimensional histogram $H(\vec{\omega})$, and the acceptance is calculated as the ratio of accepted and generated events in each three-dimensional bin in $\vec{\omega}$ divided by the total number of generated events such that the sum of the weights in all the bins in the histogram is 1. Thus, the acceptance function can be interpreted as the probability to find an event at each position in the $\vec{\omega}$ space. The projections of $H(\vec{\omega})$ in the three helicity (transversity) angles are shown in FIG. 6 for $B_s^0 \to \phi\phi$ (in FIG.7 for $B_s^0 \to J/\psi\phi$).

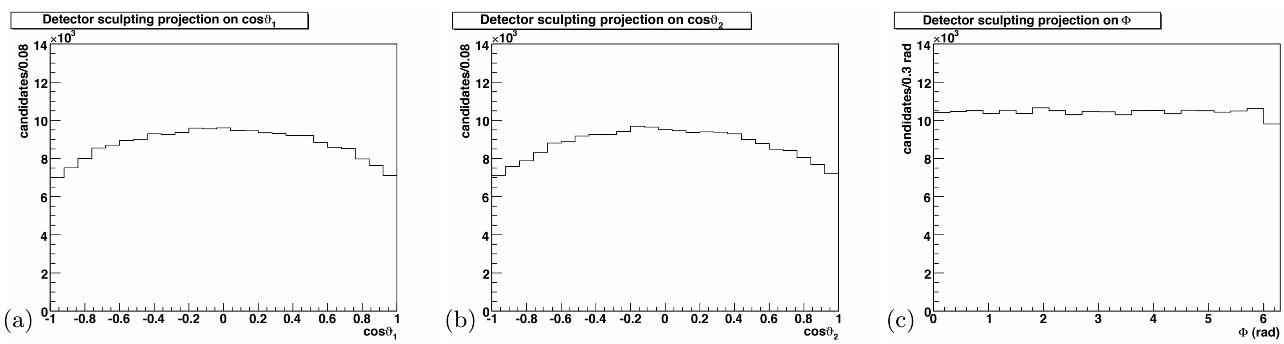

FIG. 6: Detector angular acceptance projections for $B_s^0 \to \phi\phi$: $\cos\vartheta_1$ (a), $\cos\vartheta_2$ (b) and Φ (c).

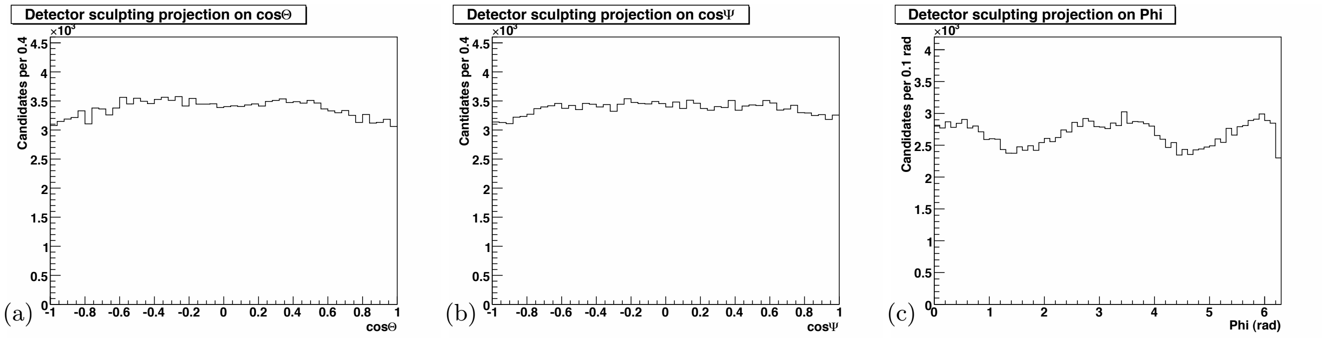

FIG. 7: Detector angular acceptance projections for $B_s^0 \rightarrow J/\psi\phi$: $\cos\Theta$ (a), $\cos\Psi$ (b) and Φ (c).

The angular acceptance effect is finally taken into account by the multiplicative term $\mathcal{H}(\vec{\omega})$ in the signal angular pdf:

$$g_{\rm s}^{(\omega)} = \frac{d^3\Lambda(\vec{\omega})}{d\vec{\omega}} \rightarrow g_{\rm s}^{(\omega)} = \frac{1}{\mathcal{N}}\frac{d^3\Lambda(\vec{\omega})}{d\vec{\omega}}\mathcal{H}(\vec{\omega}) \tag{14}$$

where $\mathcal{N}$ is a normalization term.

Finally, we use a purely empirical parametrization derived by analysing the angular distributions in the mass sidebands to model the background. Assuming that the background pdf factorizes for the three angles, the pdf is a constant in the ϕ angle and is parameterized as $1 + B\cos^2\vartheta$ for the ϑ_1 and ϑ_2.

C. Fit Tests

Before carrying out the fit over the data sample of $B_s^0 \rightarrow \phi\phi$, we perform several tests. The aim is to validate the correctness of the implementation, to investigate the likelihood behavior as function of the parameters, to look at their resolutions and to detect any potential fit biases. The tests that we perform are:

1. the pulls distributions;
2. the fit of $B_s^0 \rightarrow J/\psi\phi$, used as a control sample;
3. the fit of the realistic MC;

1. Pulls Distributions

We generate a large set of pseudo-experiments, randomly polling the probability density function in each variable subspace to assign a value to the event variables. As a consequence, each pseudo-experiment yields a different random sample of events. For each of these pseudo-experiments, we perform a fit in the same way we do on the data. For each parameter ξ_i on the fit, the corresponding pull $\mathcal{P}_i$ is defined as:

$$\mathcal{P}_i = \frac{\xi_i^{\rm fit} - \xi_i^{\rm input}}{\sigma_i} \tag{15}$$

where $\xi_i^{\rm input}$ is the parameter assigned in the random generation of the pseudo-experiment variables, $\xi_i^{\rm fit}$ is its value found by the fitter, and σ_i is its uncertainty. In principle, the variables $\mathcal{P}_i$ are gaussian distributed, with mean and width equal to 0 and 1, respectively. Thus, if the fitter is correct, we expect to find this kind of pulls distributions.

We perform the pulls test for the fitter, generating 1000 pseudo-experiments of 480 events for each (the statistic of the actual $B_s^0 \rightarrow \phi\phi$ sample). The generation of pseudo-experiments is done using as input parameters the results of the fit performed on the actual $B_s^0 \rightarrow \phi\phi$ sample. The results of the test are satisfactory and they are shown in TAB. III, while the pulls plots are in FIG. 8.

Parameter	Input value	Avg Neg. Err	Avg Pos. Err	Mean	Variance	Prob(χ^2) [%]
M	5.364 GeV/c^2	-0.0012 GeV/c^2	0.0012 GeV/c^2	-0.03 ± 0.03	1.04 ± 0.02	91
σ	0.016 GeV/c^2	-0.0010 GeV/c^2	0.0010 GeV/c^2	-0.05 ± 0.03	1.04 ± 0.02	95
$f_{\rm b}$	0.38	-0.03	0.03	-0.07 ± 0.03	1.04 ± 0.02	62
b	2.7 c^2/GeV	-0.7 c^2/GeV	0.7 c^2/GeV	-0.03 ± 0.03	0.97 ± 0.02	86
$\lvert A_0\rvert^2$	0.35	-0.040	0.040	0.03 ± 0.03	0.93 ± 0.02	62
$\lvert A_\parallel\rvert^2$	0.29	-0.039	0.039	0.06 ± 0.03	0.99 ± 0.02	22
$\cos\delta_\parallel$	-0.90	-0.15	0.18	-0.02 ± 0.03	1.10 ± 0.02	0
B	0.5	-0.27	0.30	0.02 ± 0.03	0.98 ± 0.02	3

TABLE III: Pulls mean and variance for $B_s^0 \to \phi\phi$ (480 events per pseudo-experiment). In the second column the input parameters of the generation are listed. The third column reports the average negative error in the pseudo-experiments fit, while the fourth column shows the average positive error. The fifth and the sixth columns list the mean value and the variance of the pull distributions, respectively. The seventh column presents the χ^2 probability for a gaussian fit of the pulls distribution with mean and variance 0 and 1, respectively.

2. *Fit to the Displaced Tracks $B_s^0 \to J/\psi\phi$ Sample*

We use the $B_s^0 \to J/\psi\phi$ decay mode as a control sample: we compare the results coming from our fit with the ones obtained in the different analysis published in [1], whose events was collected at CDF II by a different trigger selection, the Dimuon trigger. Therefore, the control sample serves the purpose of improving the reliability of the main analysis. For its intrinsic nature of control sample, many of the technical aspects are in common with the $B_s^0 \to \phi\phi$ analysis. The main difference is that the $B_s^0 \to J/\psi\phi$ decay is described making use of the transversity angles $\vec{\Omega} = (\Theta, \Psi, \Phi)$.

The results of the fit performed on 2.9 fb^{-1}of data for the $B_s^0 \to J/\psi\phi$ are listed in the TAB. IV, and the fit projections onto the three transversity angles are shown in fig. 9. We compare the results with the ones obtained in the analysis published in [1], whose data were collected by the CDF II detector between February 2002 and January 2007, and correspond to an integrated luminosity of 1.7 fb^{-1}. The fit results are in agreement with the ones published in [1]. In conclusion, the two experiments have compatible results among each other and provide us with an important successful check of our framework on the kinematically equivalent data sample $B_s^0 \to J/\psi\phi$: this result contributes to enforce the reliability of our angular analysis implementation.

Parameter	Displaced Track sample	Dimuon sample
$\lvert A_0\rvert^2$	0.534 ± 0.019(stat)	0.531 ± 0.020(stat) ± 0.007(syst)
$\lvert A_\parallel\rvert^2$	0.220 ± 0.025(stat)	0.239 ± 0.029(stat) ± 0.011(syst)

TABLE IV: Comparison of our fit results and the ones in [1] for $B_s^0 \to J/\psi\phi$.

3. *Fit to the Realistic MC*

The fit to the realistic MC data sample is the third test that we present. The MC is called "realistic" because it reproduces in order the main physical processes and the processing steps involved in collecting data from real p$\bar{\rm p}$ interactions. The purpose of the test is to check if the fit is reliable. This means that the fit should return the same set of parameters adopted in the MC generation of the events. We produce and fit three realistic MC samples, with different polarization values in the generation. The results are all satisfactory:

i) 21000 events		
Parameter	generated value	fitted value
$\lvert A_0\rvert^2$	0.48	0.4815±0.0042
$\lvert A_\parallel\rvert^2$	0.28	0.2824±0.0041
$\delta_\parallel$ [rad]	0.742	0.735±0.019

ii) 12000 events		
Parameter	generated value	fitted value
$\lvert A_0\rvert^2$	0.81	0.8191±0.0039
$\lvert A_\parallel\rvert^2$	0.15	0.1436±0.0037
$\delta_\parallel$ [rad]	0.442	0.437±0.033

iii) 240000 events		
Parameter	generated value	fitted value
$\lvert A_0\rvert^2$	0.333	0.3276±0.0013
$\lvert A_\parallel\rvert^2$	0.333	0.3344±0.0014
$\delta_\parallel$ [rad]	1.571	1.5667±0.051

D. Fit Results for Real Data

The results of the fit performed on 2.9 fb^{-1}of data for the $B_s^0 \to \phi\phi$ are finally listed in the TAB. V (a) and the correlation coefficients are listed in TAB. V (b). Note that the fit estimates for $\cos\delta_\parallel$ is in the physical region. The fit projections onto the three helicity angles are shown in FIG. 10: we see that the data distributions are very well reproduced by the fitting functions.

Parameter	Fit value
M [GeV/c^2]	5.3636 ± 0.0012
σ [GeV/c^2]	0.0165 ± 0.0011
$f_{\rm b}$	0.381 ± 0.030
b [c^2/GeV]	2.68 ± 0.67
$\lvert A_0\rvert^2$	0.348 ± 0.041
$\lvert A_\parallel\rvert^2$	0.287 ± 0.043
$\cos\delta_\parallel$	$-0.91^{+0.15}_{-0.13}$
B	$0.49^{+0.31}_{-0.26}$

(a) Results of the fit.

	M	σ	$f_{\rm b}$	b	$\lvert A_0\rvert^2$	$\lvert A_\parallel\rvert^2$	$\cos\delta_\parallel$	B
M	+1.000	−0.047	+0.049	+0.070	+0.002	−0.008	−0.010	+0.010
σ	−0.047	+1.000	−0.357	−0.022	+0.055	−0.025	+0.110	+0.036
$f_{\rm b}$	+0.029	−0.357	+1.000	+0.020	−0.064	+0.023	−0.147	−0.034
b	+0.070	−0.022	+0.020	+1.000	−0.005	−0.002	−0.000	+0.003
$\lvert A_0\rvert^2$	+0.002	+0.055	−0.064	−0.005	+1.000	−0.447	+0.133	−0.217
$\lvert A_\parallel\rvert^2$	−0.008	−0.025	+0.023	−0.002	−0.447	+1.000	+0.092	+0.106
$\cos\delta_\parallel$	−0.010	+0.110	−0.147	−0.000	+0.133	+0.092	+1.000	+0.025
B	+0.010	+0.036	−0.034	+0.003	−0.217	+0.106	−0.025	+1.000

(b) Correlation coefficients.

TABLE V: $B_s^0 \to \phi\phi$ fit.

The contour-plots for the three polarization parameters are shown in fig. 11. These contour-plots provide the actual coordinates of the points around the contour calculated at the level $-2\log(\mathcal{L}(\vec{\xi}_{\rm min}))+2.3$ which corresponds to the Confidence Level of 68.3%.

VII. SYSTEMATIC UNCERTAINTIES

The systematic uncertainty for the ML fit is meant to cover the effects which may have not been properly incorporated in our model and could precisely lead to systematic biases on the estimates. We consider the following systematic sources.

Residual discrepancy Data-MC. In the MC validation performed in the branching ratio analysis [21], we saw a small discrepancy between the data and MC $p_{\rm T}(B)$ distribution. Then, we find a reweighing function (see [21]) and we reweigh the 3D histogram of angular signal acceptance in the final fit. We evaluate how this changes the fit estimates.

Binning of angular acceptance histogram. Since the signal angular acceptance is taken from a 3D histogram, we want to know if there is a dependence of the fit estimates on its binning.

Angular acceptance model (Trigger-Paths division). Since we fill the angular acceptance histogram with the events coming from the sum of the three exclusive trigger-paths data set, we consider the potential bias introduced by the trigger differences in the angular acceptance model.

Angular background model. We study the impact of the specific angular background model used with respect to different parameterizations.

Reflection background component. In the fit we do not include the $B_d^0 \to \phi K^\star$ reflection component. Anyway, we already know its fraction in our data sample from the branching ratio analysis. We evaluate the impact of such an effect on the polarization estimates.

***ct*-dependence of angular acceptance.** We estimate the impact on the fit estimates of some detector angular acceptance dependences on ct.

Satellite Peak. We evaluate the effect of potential reflections or other peaking background that might be hiding on the low mass side of the signal peak.

Non-resonant contribution. We account for possible small S-wave (scalar) contribution to the angular distribution, due to non-resonant components under the ϕ peak signal, or a resonant contribution such as a $f_0\phi$ final state. We decided to generate MC for two possible (main) S-wave contribution that might leak under our signal:

1. B_s^0 to ϕ and a non resonant pair of Kaons ($B_s^0 \to \phi(K^+K^-)$);
2. B_s^0 to ϕ and an f_0 which in turn decays into the K^+K^- channel ($B_s^0 \to \phi f_0$).

We normalize the fraction of such contributions with respect to the signal yield considering the analogy with the B_d^0 case; we estimate that the possible contribution of these backgrounds in our sample are 0.9 % for the $B_s^0 \to \phi(K^+K^-)$ and 4.6% for the $B_s^0 \to \phi f_0$.

Dependence of the Angular Acceptance on $\Delta\Gamma_s$. If the width difference $\Delta\Gamma_s$is sizable (as expected and verified experimentally) a significant bias on the polarization at $t = 0$ (the physical observable) is expected when performing a time integrated measurement. Assuming world average value for $\Gamma_{\rm H}$ and $\Gamma_{\rm L}$, we evaluate the effect coming purely from the normalization of the decay rate; we need to consider the effect induced by a non uniform acceptance with the B^0_s decay proper time introduced by the two displaced track trigger as well. The realistic MC reproduces the ct acceptance of the trigger and selection reasonably well for the purpose we are interested here, see e.g. FIG. 12. Thus, the related experimental systematic uncertainty is evaluated with MC method.

$\tau_{\rm L}$ and $\tau_{\rm H}$ uncertainties We consider the propagation of the $\tau_{\rm L(H)}$ uncertainties to the polarization amplitudes.

CP-violation dependence. In our fit we assume to be in the SM, thus, we fix the CP-violation $\phi_{\rm s} = 0$. We evaluate how this assumptions affect the fit estimates.

We summarize the systematic uncertainties in the following table

	$\lvert A_0\rvert^2$ syst	$\lvert A_\parallel\rvert^2$ syst	$\lvert A_\perp\rvert^2$ syst	$\cos\delta_\parallel$ syst
MC reweight	±0.003	±0.001	±0.002	±0.007
Acceptance binning	±0.001	±0.001	±0.000	±0.004
Acceptance Model	±0.005	±0.002	±0.003	±0.005
Background Model	±0.001	±0.001	±0.002	±0.009
Acceptance ct-dependence	±0.000	±0.001	±0.001	±0.004
Reflection component	±0.008	±0.002	±0.006	±0.019
Non-resonant contribution	±0.013	±0.003	±0.010	±0.084
Satellite peak	±0.004	±0.000	±0.004	±0.020
Acceptance $\Delta\Gamma$-dependence	±0.009	±0.009	±0.016	±0.011
$\tau_{\rm L(H)}$ uncertainties	±0.008	±0.006	±0.017	
CP-violation	±0.002	±0.001	±0.003	±0.009
total	±0.021	±0.011	±0.027	±0.090

VIII. FINAL RESULTS AND CONCLUSIONS

We have presented the first measurement of the polarization amplitudes for the charmless $B^0_s \to \phi\phi \to [K^+K^-][K^+K^-]$ decay of the B^0_s meson. The results for the polarization amplitudes and the cosine of the strong parallel phase are:

$$
\begin{aligned}
|A_0|^2 &= 0.348 \pm 0.041(\text{stat}) \pm 0.021(\text{syst})\\
|A_\parallel|^2 &= 0.287 \pm 0.043(\text{stat}) \pm 0.011(\text{syst})\\
|A_\perp|^2 &= 0.365 \pm 0.044(\text{stat}) \pm 0.027(\text{syst})\\
\cos\delta_\parallel &= -0.91^{+0.15}_{-0.13}(\text{stat}) \pm 0.09(\text{syst})
\end{aligned}
$$

and the resulting polarization fractions are:

$$
\begin{aligned}
f_{\rm L} &= 0.348 \pm 0.041(\text{stat}) \pm 0.021(\text{syst})\\
f_{\rm T} &= 0.652 \pm 0.041(\text{stat}) \pm 0.021(\text{syst})
\end{aligned}
$$

A. Theoretical Considerations on the Results

From the measurement we draw the consideration that the the amplitude hierarchy $|A_0| \gg |A_\parallel| \simeq |A_\perp|$ of the SM is disfavored in the $B_s \to \phi\phi$ decay, being $|A_0| \simeq |A_\perp| \gtrsim |A_\parallel|$; this is similar to the measurements for the $\bar{b} \to \bar{s}$ penguin transition of $B \to \phi K^\star$ decays [8, 25, 26], which were the origin of the "polarization puzzle".

We compare our results with the theoretical predictions of the various approaches adopted in the calculation of the polarization amplitudes. They are reported in tab. VI. We find that our central values are consistent within the uncertainty ranges with the expectations of the QCD factorization 1 and 2 in [2], while they are not with the expectation of perturbative QCD [27].

	$f_{\rm L}$ [%]	$f_{\rm T}$ [%]
CDF Run II	$34.8 \pm 4.1(\text{stat}) \pm 2.1(\text{syst})$	$65.2 \pm 4.1(\text{stat}) \pm 2.1(\text{syst})$
QCD factorization 1	48^{+0+26}_{-0-27}	52^{+0+26}_{-0-27}
QCD factorization 2	34 ± 28	66 ± 28
QCD factorization 3	86.6	13.4
Naive factorization	88.3	11.7
NLO EWP 1	86.3	13.7
NLO EWP 2	86.3	13.7
perturbative QCD	$61.9^{+3.6+2.5+0.0}_{-3.2-3.3-0.0}$	$38.1^{+3.6+2.5+0.0}_{-3.2-3.3-0.0}$

TABLE VI: $B_s \to \phi\phi$ polarization amplitudes: comparison with theoretical predictions. $f_{\rm L}$ and $f_{\rm T}$ are the fraction of longitudinal and transverse polarisation, respectively. The references are: [2] for QCD factorization 1, [**?**] for QCD factorization 2, [28] for QCD factorization 3 and Naive factorization, [29] for NLO EWP 1 and 2, [27] for perturbative QCD.

Acknowledgments

We thank the Fermilab staff and the technical staffs of the participating institutions for their vital contributions. This work was supported by the U.S. Department of Energy and National Science Foundation; the Italian Istituto Nazionale di Fisica Nucleare; the Ministry of Education, Culture, Sports, Science and Technology of Japan; the Natural Sciences and Engineering Research Council of Canada; the National Science Council of the Republic of China; the Swiss National Science Foundation; the A.P. Sloan Foundation; the Bundesministerium für Bildung und Forschung, Germany; the World Class University Program, the National Research Foundation of Korea; the Science and Technology Facilities Council and the Royal Society, UK; the Institut National de Physique Nucleaire et Physique des Particules/CNRS; the Russian Foundation for Basic Research; the Ministerio de Ciencia e Innovación, and Programa Consolider-Ingenio 2010, Spain; the Slovak R&D Agency; and the Academy of Finland.

[1] CDF Collaboration: T. Aaltonen. Measurement of Lifetime and Decay-Width Difference in $B^0_s \to J/\psi\phi$ Decays. *Physical Review Letters*, 100:121803, 2008.
[2] Martin Beneke and Johannes Rohrer and Deshan Yang. Branching fractions, polarisation and asymmetries of $B \to VV$ decays. *Nuclear Physics B*, 774(1-3):64 – 101, 2007.
[3] Belle Collaboration. *Phys. Rev. Lett.*, 96:171801, 2006.
[4] B. Aubert et al. A Study of $B^0 \to \rho^+\rho^-$ Decays and Constraints on the CKM Angle alpha. *Physical Review D*, 76:052007, 2007.
[5] *BABAR* Collaboration. Measurements of Branching Fraction, Polarization, and Charge Asymmetry of $B^\pm \to \rho^\pm\rho^0$ and a Search for $B^\pm \to \rho^\pm f^0(980)$. *Physical Review Letters*, 97(26):261801, 2006.
[6] *BABAR* Collaboration. b meson decays to $\omega k^\star$, $\omega\rho$, $\omega\omega$, $\omega\phi$, and ωf^0. *Physical Review D (Particles and Fields)*, 74(5):051102, 2006.
[7] *BABAR* Collaboration. Evidence for $B^0 \to \rho^0\rho^0$ Decays and Implications for the Cabibbo-Kobayashi-Maskawa Angle α . *Physical Review Letters*, 98(11):111801, 2007.
[8] The BABAR Collaboration and B. Aubert. Vector-Tensor and Vector-Vector Decay Amplitude Analysis of $B^0 \to \phi K^\star$. *Physical Review Letters*, 98:051801, 2007.
[9] The BABAR Collaboration and B. Aubert. Measurements of Branching Fractions, Polarizations, and Direct CP-Violation Asymmetries in $B \to \rho K^\star$ and $B \to f^0(980)K^\star$ Decays. *Physical Review Letters*, 97(20):201801, 2006.
[10] K. F. Chen and for the Belle Collaboration. Measurement of Polarization and Triple-Product Correlations in $B \to \phi K^\star$ Decays. *Physical Review Letters*, 94:221804, 2005.
[11] Ezequiel Alvarez, Luis N. Epele, Daniel Gomez Dumm, and Alejandro Szynkman. Right handed currents and FSI phases in $B^0 \to \phi K^{\star 0}$. *Physical Review D*, 70:115014, 2004.
[12] C. S. Kim and Ya-Dong Yang. Polarization Anomaly in $B \to \phi K^{\star 0}$ and Probe of Tensor Interactions, 2004.
[13] A. Ali, G. Kramer, Y. Li, C.-D. Lü, Y.-L. Shen, W. Wang, and Y.-M. Wang. Charmless nonleptonic B_s decays to PP, PV, and VV final states in the perturbative QCD approach. *Physical Review D*, 76(7):074018–+, October 2007.
[14] Alexander L. Kagan. Polarization in B –¿ V V decays. *Phys. Lett.*, B601:151–163, 2004.
[15] P. Colangelo, F. De Fazio, and T. N. Pham. The riddle of polarization in B –¿ V V transitions. *Phys. Lett.*, B597:291–298, 2004.
[16] Massimo Ladisa, Vincenzo Laporta, Giuseppe Nardulli, and Pietro Santorelli. Final state interactions for B –¿ V V charmless decays. *Phys. Rev.*, D70:114025, 2004.
[17] Hai-Yang Cheng, Chun-Khiang Chua, and Amarjit Soni. Final state interactions in hadronic B decays. *Phys. Rev.*, D71:014030, 2005.
[18] Christian W. Bauer, Dan Pirjol, Ira Z. Rothstein, and Iain W. Stewart. B –¿ M(1) M(2): Factorization, charming penguins,

strong phases, and polarization. *Phys. Rev.*, D70:054015, 2004.
[19] Alakabha Datta, David London, Joaquim Matias, Makiko Nagashima, and Alejandro Szynkman. Final-state Polarization in Bs Decays. *Eur. Phys. J.*, C60:279–284, 2009.
[20] CDF Collaboration and D. Acosta. First Evidence for $B_s^0 \to \phi\phi$ Decay and Measurements of Branching Ratio and A_{CP} for $B^+ \to \phi K^+$. *Physical Review Letters*, 95:031801, 2005.
[21] The CDF collaboration. Updated Measurement of the $B_s \to \phi\phi$ Branching Ratio Using 2.9 fb^{-1}. *CDF Public Note*, 10064, 2010. unpublished.
[22] C. Amsler et al. Particle Data Group. *Physics Letters B*, 667, 2008 and 2009 partial update for the 2010 edition.
[23] The BABAR Collaboration and B. Aubert . Measurement of the $B \to \phi K^\star$ Decay Amplitudes. *Phys. Rev. Lett.*, 93(23):231804, Dec 2004.
[24] E. J. Thomson et al. Online Track Processor for the CDF Upgrade. *IEEE Trans. Nucl. Sci.*, 49, 2002.
[25] Belle Collaboration. Evidence for Neutral B Meson Decays to omega $K^{\star 0}$. *Physical Review Letters*, 101(23):231801, 2008.
[26] *BABAR* Collaboration. Amplitude Analysis of the $B^\pm \to \phi K^{\star\pm}(892)$ Decay. *Physical Review Letters*, 99(20):201802, 2007.
[27] Ahmed Ali, Gustav Kramer, Ying Li, Cai-Dian Lu, Yue long Shen, Wei Wang, and Yu-Ming Wang. Charmless non-leptonic B_s decays to PP, PV and VV final states in the pQCD approach. *Physical Review D*, 76:074018, 2007.
[28] Xinqiang Li, Gongru Lu, and Yadong Yang. Charmless $\bar{B}_s \to VV$ Decays in QCD Factorization. *ERRATUM-IBID.D*, 71:019902, 2005.
[29] D. Du and L. Guo. *J. Phys. G: Nucl. Part. Phys.*, 23:525, 1997.
[30] In fact, for two spin 1 particles, L can be equal to 0, 1, or 2 to obtain the spin 0 initial state.
[31] Fix the following convention: if the final states are charged particles, P_1 and P_3 are the positive charged ones.
[32] We are supposing that B_s^0 and $\bar{B}_s^0$ are produced in equal numbers at the Tevatron.
[33] We evaluate the impact of this assumption in the systematics treatment.

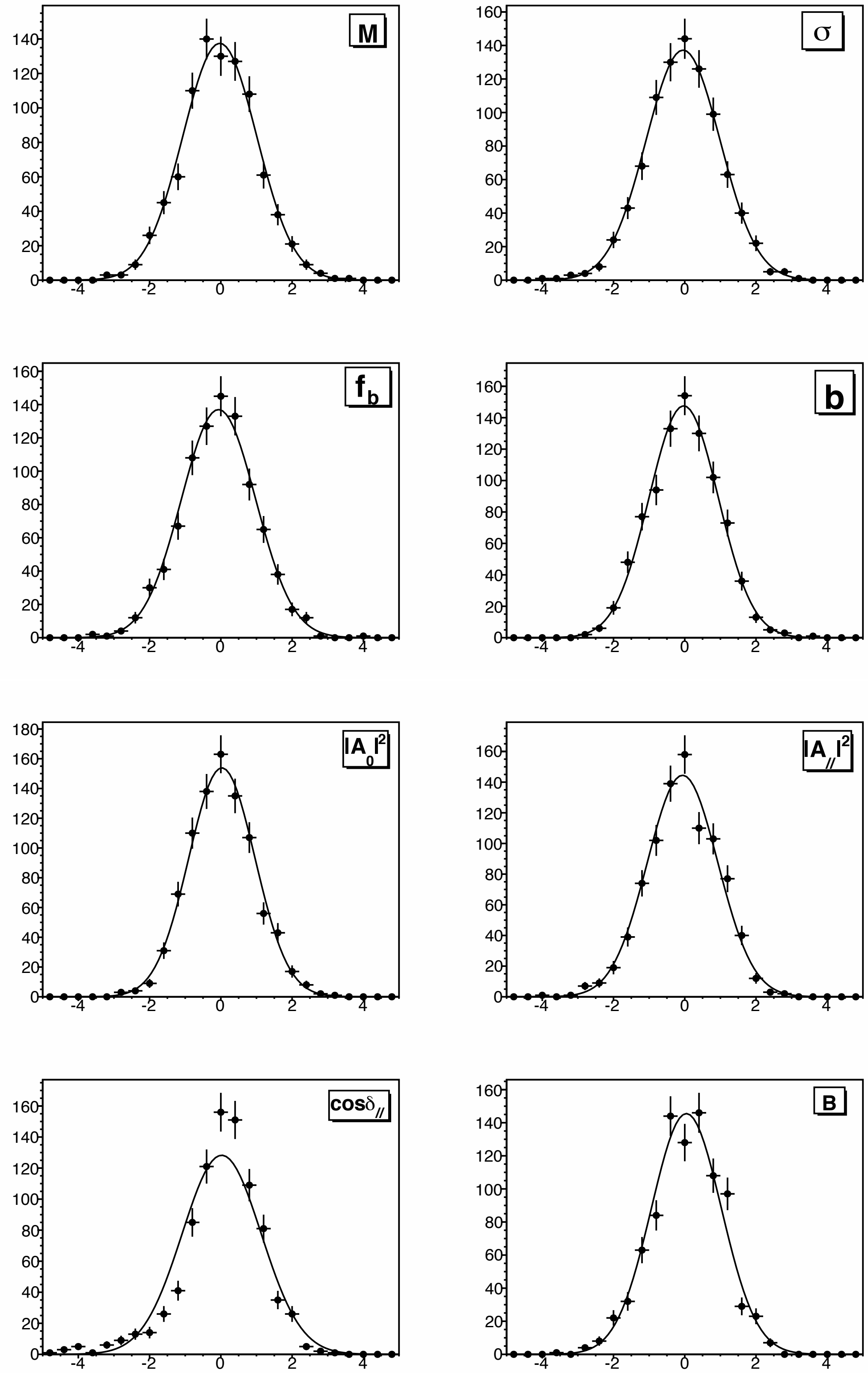

FIG. 8: Pulls distributions of fit parameters for $B_s^0 \to \phi\phi$ (480 events per pseudo-experiment).

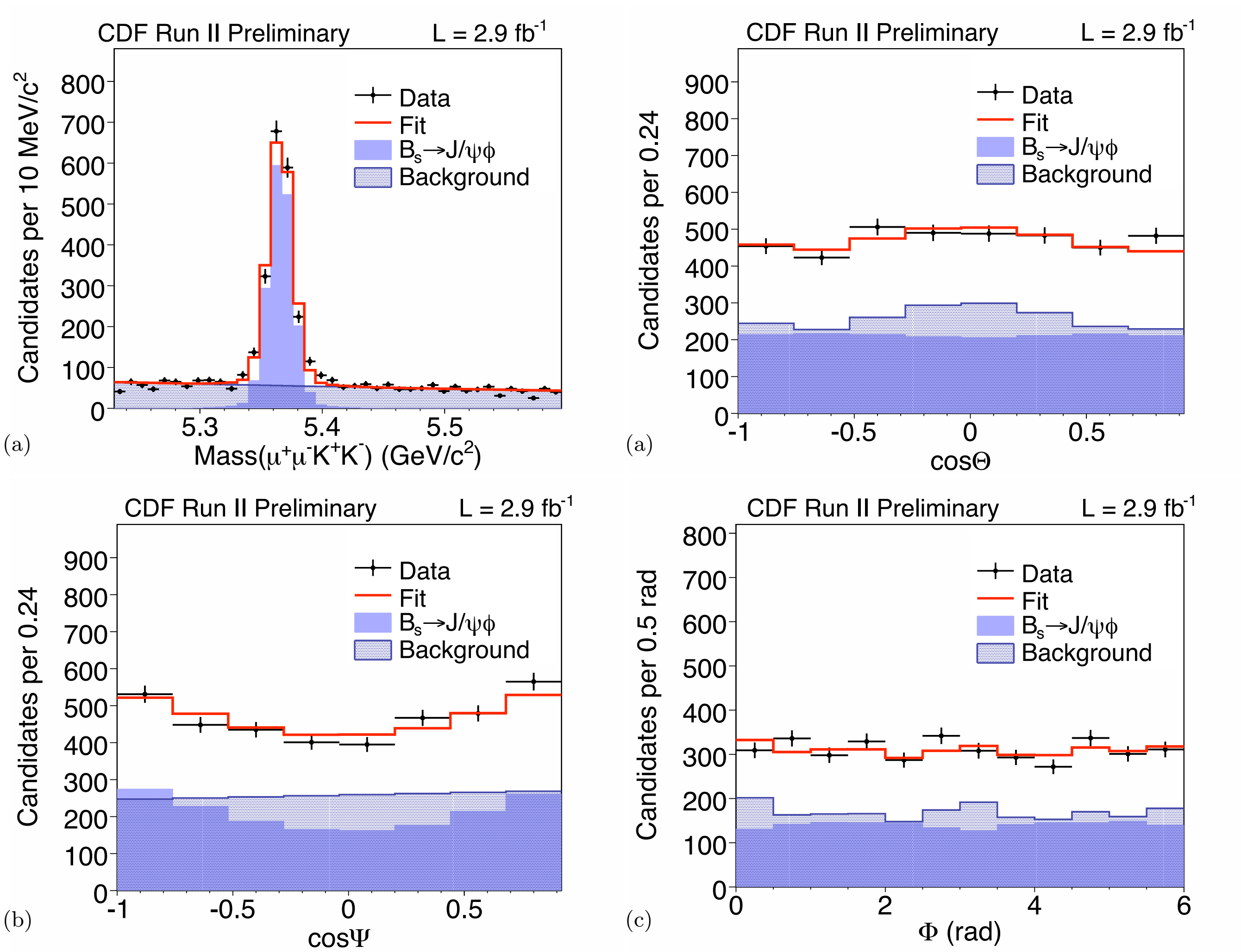

FIG. 9: Angular fit projections for $B_s^0 \to J/\psi\phi$: mass (s), $\cos\Theta$ (b), $\cos\Psi$ (c) and Φ (d).

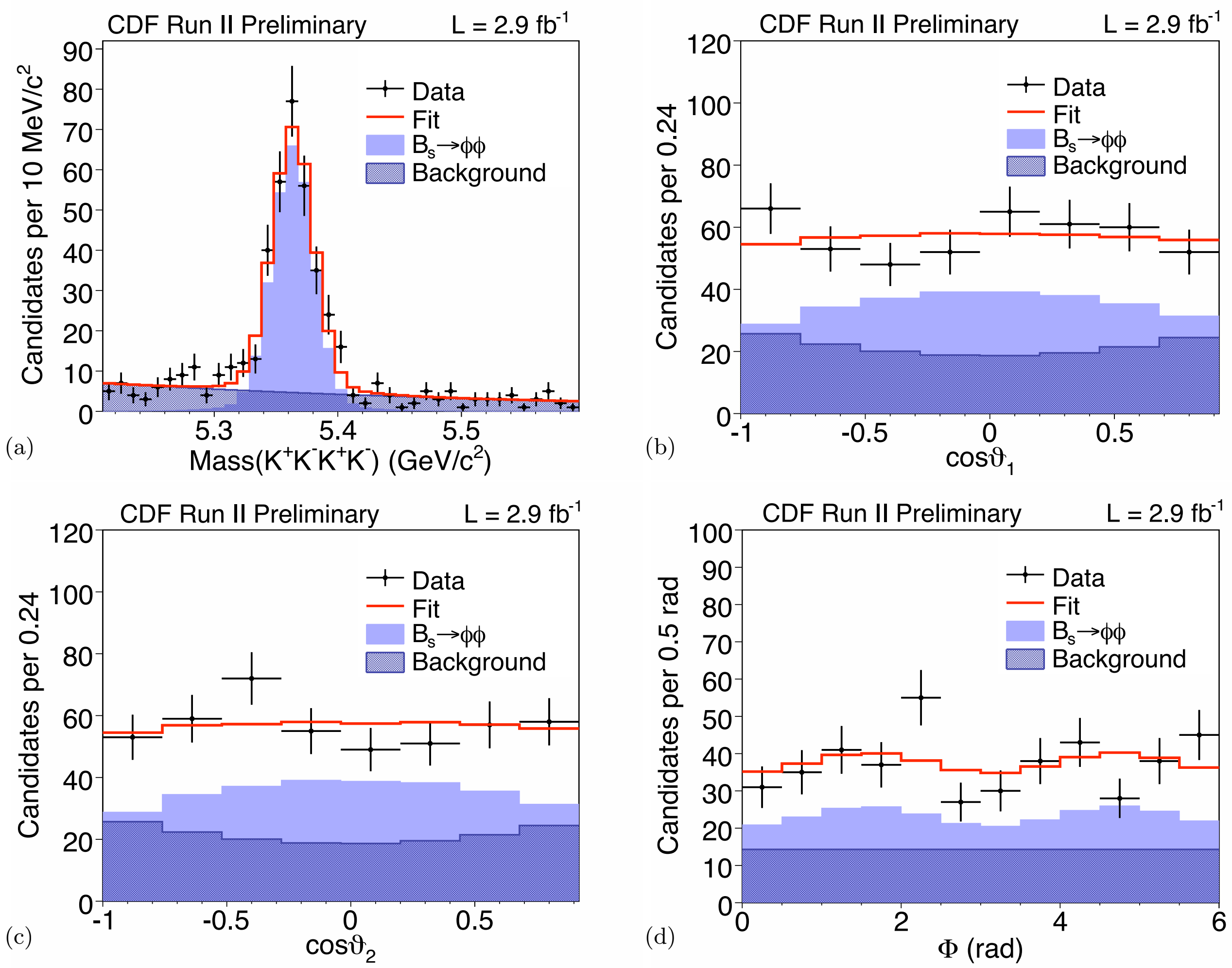

FIG. 10: Projections of the fit for $B_s^0 \to \phi\phi$: mass (a), $\cos\vartheta_1$ (b), $\cos\vartheta_2$ (c) and Φ (d).

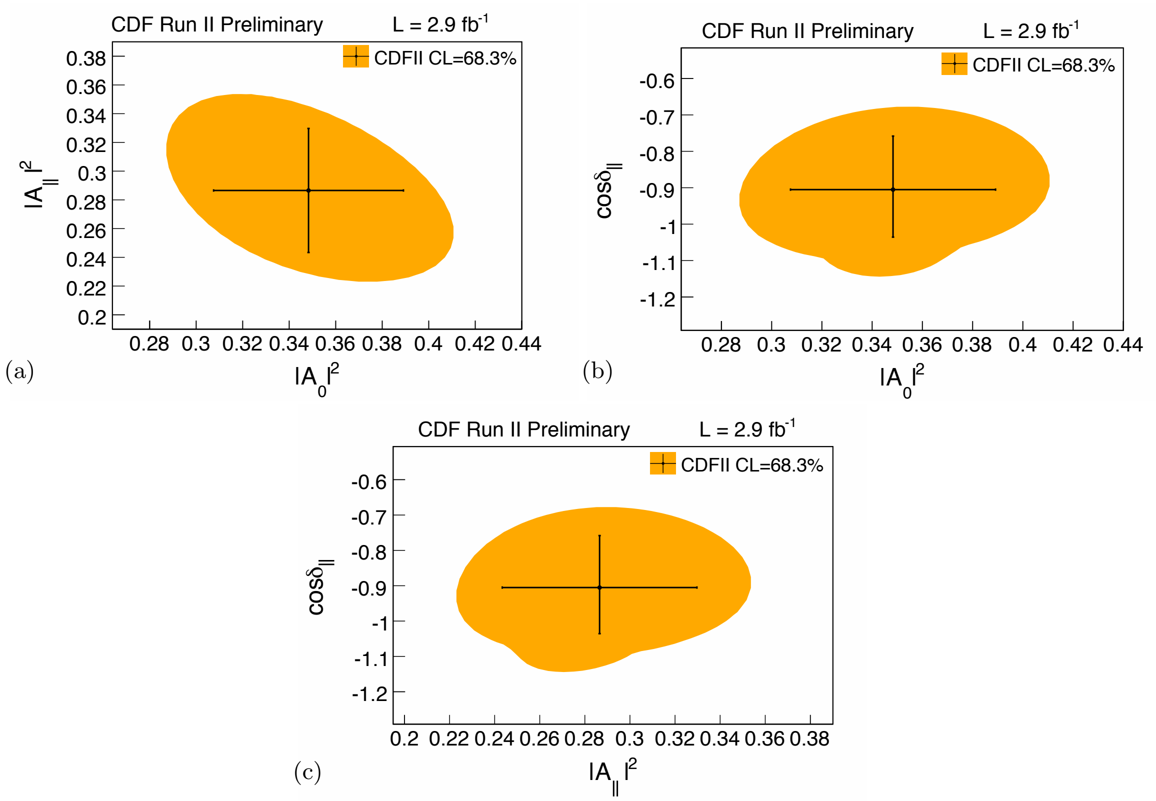

FIG. 11: Contour-plots of the fit for $B_s^0 \to \phi\phi$: $|A_0|^2$ versus $|A_\parallel|^2$ (a), $|A_0|^2$ versus $\cos\delta_\parallel$ (b) and $|A_\parallel|^2$ versus $\cos\delta_\parallel$ (c).

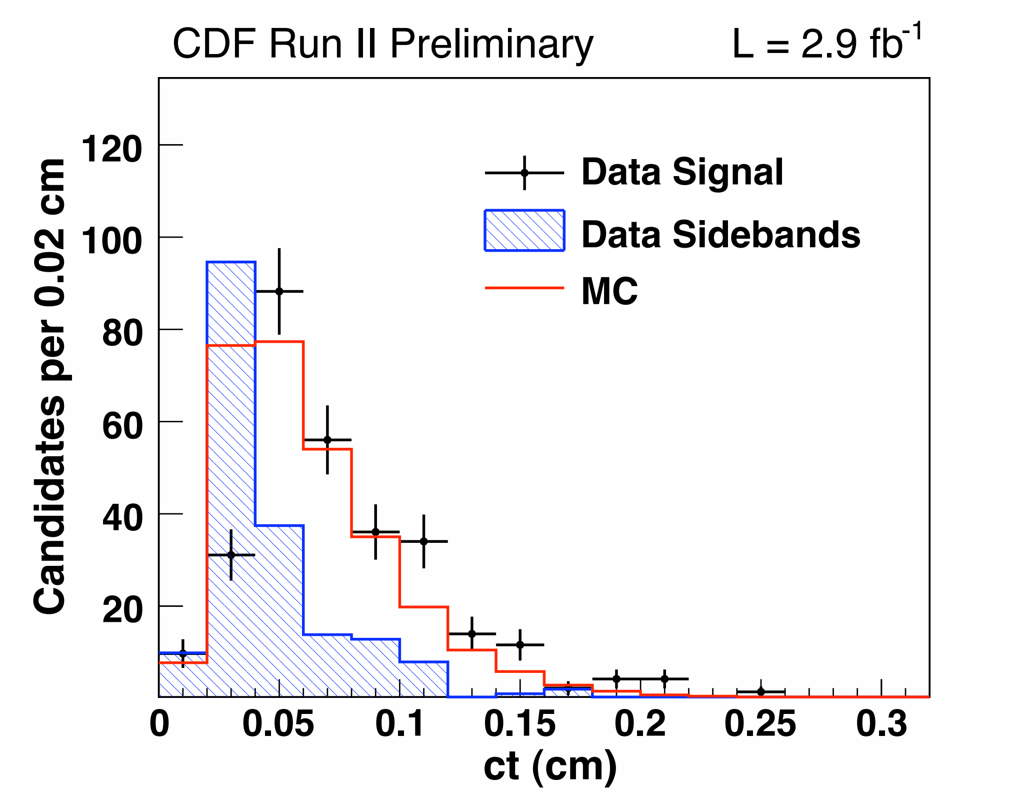

FIG. 12: Reconstructed proper time ct for sideband subtracted signal compared with MC expectation

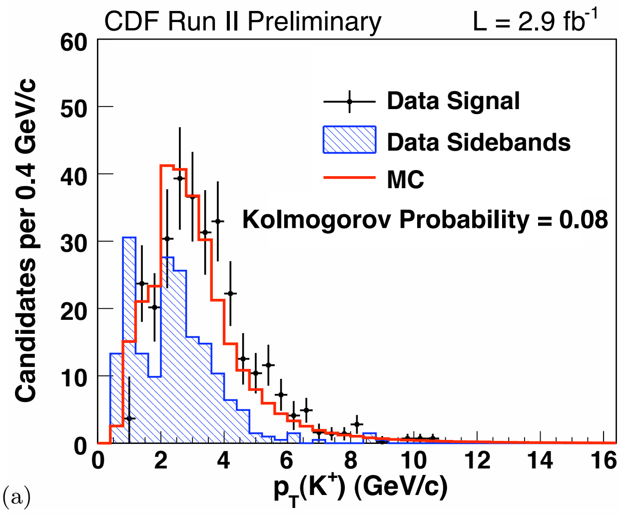

(a)

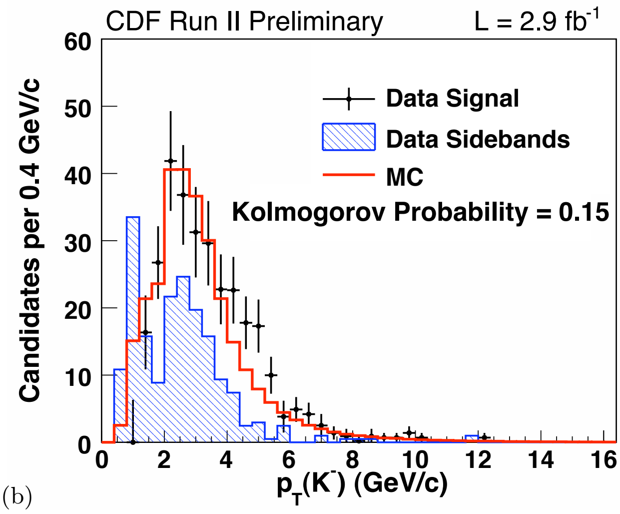

(b)

FIG. 13: p_T distribution for the K^+ (a) and K^- (b) particles for the $B_s^0 \to \phi\phi$. The black points are side-bands subtracted data (see Sect. **??**); the red line is the reweighted MC; the red dotted line is the not-reweighted MC; the blue histogram is the sidebands data distribution. The Kolmogorov probability for the comparison of Data and the reweighted MC distributions is 0.08 for (a) and it is 0.15 for (b).